A method of determination of electrical conduction mechanisms in complex amorphous materials

P. Kupracz[a,1], N. A. Wójcik[a,b], R. J. Barczyński[a]

[a]Faculty of Applied Physics and Mathematics, Gdańsk University of Technology, ul. Narutowicza 11/12, 80-233 Gdańsk, Poland

[b] Department of Built Environment and Energy Technology, Linnaeus University, 35195 Växjö, Sweden

Abstract

A novel approach to determine conduction mechanisms in complex amorphous materials was presented and tested on a real system. According to the method, total electrical admittance of the material is separated to a couple of processes, which can be described by Jonscher's universal dielectric response. In the next step, a temperature dependency of dielectric response parameters of each process is determined and compared with known models of conduction mechanisms in structural amorphous materials. Using this approach, a presence of two different conduction mechanisms describing electrical conductivity in a system was described.

Keywords:
Impedance spectroscopy, Glass, Polaron Hopping, Admittance, Electrical properties analysis

1. Introduction

One of the characteristic properties of dielectric materials is a strong dispersion of the ac conductance (Y'). At low frequencies, one observes a frequency-independent dc conductance (Y_{dc}), while at higher frequencies conductance usually varies as a power of the frequency, what overall may be written as Eq. 1:

$$Y'(\omega) = Y_{dc} + A\omega^n, \tag{1}$$

where $\omega = 2\pi f$ is an angular frequency, and parameters A and n can be temperature dependent. The increase in conductance usually continues up to phonon frequency ($\omega_{ph} \approx 10^{12}\,s^{-1}$) [1].

In a series of publications, Jonsher [1–4] proposed and demonstrated the utility of Eq. 1 in order to analyze the ac conductivity in amorphous systems. This relation found application in almost every disorder solid and therefore it was named as an *universal dielectric response* (UDR). Further, it has been found [4] that UDR (Eq. 1) may be written in a full complex form in terms of admittance (Y*) as:

$$Y^*(\omega) = Y_0[1 + (j\omega\tau)^n] = Y_0\left[(\omega\tau)^n\left(cos\left(n\frac{\pi}{2}\right) + jsin\left(n\frac{\pi}{2}\right)\right)\right], \tag{2}$$

1   Corresponding author
Email addresses: piotr.kupracz@pg.edu.pl (P. Kupracz), natalia.wojcik@pg.edu.pl (N. A. Wójcik),
ryszard.barczynski@pg.edu.pl (R. J. Barczyński)

where j is an imaginary unit, τ is a relaxation time of a conduction process and exponent parameter n is less than one. The relaxation time τ is often replaced by a relaxation frequency ($\omega_0 = \tau^{-1}$) of charge carrier hopping between active sites. It can be seen, that a real part of Eq. 2 is equal to Eq. 1.

Much effort was done to create theoretical models, which explain the frequency and temperature dependencies of electrical properties. Widely accepted models [5, 6] are based on an assumption that a charge carrier moves between localized sites separated by finite distances and energy barrier potentials. There are several popular models of electrical charge transport, which describe the conductivity behavior of amorphous materials: small polaron hopping (SPH) [8], overlapping large polaron hopping (OLPH) [9,10], correlated barrier hopping (CBH) [11], quantum mechanical tunneling (QMT) [9] and continuous time random walk (CTRW) [12,13]. For every of mentioned models, Elliott [6] calculated temperature dependency of the exponential factor n (Eq. 1). According to his calculations [6], parameter n for QMT and CTWR models should be temperature independent, while with an increase in temperature it should decrease for CBH or increase for SPH. Only for OLPH exponential factor n may increase or decrease with increase in temperature depending on conduction process parameters (like polaron radius, activation energy and decay of electron wave function). Since, in many materials [5-7] the exponential factor n, obtained by fitting admittance to Eq.2, is temperature dependent, it is possible to determine conduction process mechanisms by comparing experimentally obtained $n = f(T)$ function with modeled functions [14].

Usually, to determine electrical properties of different relaxation processes, the admittance of the system is modeled by equivalent electrical circuits composed of discrete components like resistors, capacitors, constant phase elements (CPE) or Warburg's elements. Although these elements can be arranged in many different configurations, two of them are commonly used i.e., Voigt and Maxwell networks (Fig. 1a and Fig. 1b respectively) [7]. Depending on the configuration, different information about the same analyzed system can be evaluated. For instance in Voigt network, each of R_i and CPE_i elements in the circuit can be related to certain resistance and capacitance of conducting region. In Maxwell network, the global R_1 and CPE_1 parameters may be related to resistance and capacitance of process extended to the whole system, while R_i and CPE_i (for $i>1$) refer only to the resistance and capacitance of electrical conduction process which is blocked.
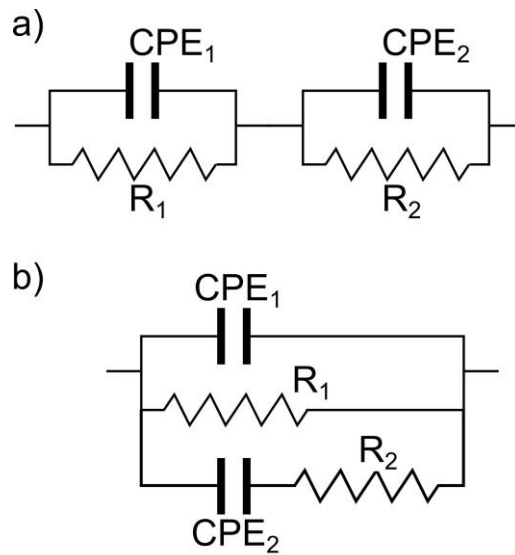

Figure 1: Scheme of simulated electrical circuits with two relaxation times: a) Voigt and b) Maxwell networks

2

A simple Voigt circuit characterized by a presence of two relaxation processes and built of two resistors and two CPEs is shown in Fig. 1a. As admittance of CPE is described by Eq. 3:

$$Y_{CPE}^*(\omega) = A(j\omega\tau)^n = A(\omega\tau)^n \left(cos\left(n\frac{\pi}{2}\right) + jsin\left(n\frac{\pi}{2}\right)\right), \qquad (3)$$

then total admittance of a single $R - CPE$ sub-circuit is defined by Eq. 4:

$$Y^*(\omega) = Y_R + Y_{CPE}^* = \frac{1}{R} + A(j\omega\tau)^n = \frac{1}{R} + A(\omega\tau)^n \left(cos\left(n\frac{\pi}{2}\right) + jsin\left(n\frac{\pi}{2}\right)\right), \qquad (4)$$

The admittance described by Jonscher's UDR equation (Eq. 2) and of a simple $R-CPE$ circuit (Eq. 4) are mathematically equivalent what has been shown by Macdonald [7]. In a consequence, the admittance of the whole Voigt circuit shown in Fig. 1a can be described by Eq. 5:

$$Y^* = \frac{Y_1^* Y_2^*}{Y_1^* + Y_2^*} = \frac{(1+R_1 A_1 (j\omega\tau_1)^{n_1})(1+R_2 A_2 (j\omega\tau_2)^{n_2})}{R_1(1+R_2 A_2 (j\omega\tau_2)^{n_2})+R_2(1+R_1 A_1 (j\omega\tau_1)^{n_1})}, \qquad (5)$$

while the admittance of equivalent Maxwell circuit (Fig. 1b) may be expressed by Eq. 6:

$$Y^* = Y_1^* + Y_2^* = \frac{1}{R_1} + A_1(j\omega\tau_1)^{n_1} + \frac{A_2(j\omega\tau_2)^{n_2}}{1+R_2 A_2 (j\omega\tau_2)^{n_2}}, \qquad (6)$$

where n_1 and n_2 are constants, τ_1 and τ_2 define a characteristic time of a relaxation processes, while $A_1 R_1 (j\omega\tau)^{n_1}$ and $A_2 R_2 (j\omega\tau)^{n_2}$ *have* unit equal to 1.

One of the examples of disordered materials, which exhibit two relaxation processes in their conductivity curves, are double-phase glasses. An interpretation of its electrical properties is especially interesting when they are produced without addition of alkali metal ions, because the most possible mechanism of charge movement in both phases is polaron hopping exhibiting different physical properties [5]. In the present article, the method of conduction mechanisms analysis is presented for any system characterized by two relaxation processes of charge transport. Next, this method was applied to a real glass system 50MnO – 30SiO$_2$ – 20B$_2$O$_3$ (in mol%) not containing alkali ions and exhibiting uniform phases separation. Finally, models accurately describing the conductivity of founded processes were determined.

2. Materials

The glass of a composition of 50MnO - 30SiO$_2$ - 20B$_2$O$_3$, was prepared using appropriate amounts of analytical grade: MnO$_2$ (Sigma-Aldrich), SiO$_2$ (POCH) and H$_3$BO$_3$ (POCH) powders. The stoichiometric composition was mixed manually in an agate mortar and heated up in a muffle furnace in a platinum crucible. The mixture was melted at 1500 K for 30 min in air. The melt was quenched by pouring on a preheated to about 500 K brass plate and pressing by another plate to obtain flat circular pellets of 1 -

1.3 mm thickness and 10 - 20 mm in the diameter. In order to study properties related to the bulk material, before a measurement, a surface layer was removed from pellets, by grinding with a dry sandpaper. Powder X-ray diffraction (XRD) measurement was done at room temperature on PANalytical X'Pert Pro MPD using the CuK_α radiation in order to check the glass structure. The microstructure of the sample was investigated with FEI Quanta 250 FEG Scanning Electron Microscope (SEM). Before measurement, glass sample was covered by a 20 nm gold layer using vacuum evaporation.

Electrical properties were examined by impedance spectroscopy measurements, which were carried out in the temperature range of 445 K - 760 K with a Novocontrol Concept 40 broadband dielectric spectrometer. The used frequency range was from 10 mHz to 1 MHz and the ac signal was 1 V_{rms}. Before the measurements, pellet of glass was polished to obtain plane parallel samples. Circular gold electrodes of 9 - 12 mm in the diameter were deposited by vacuum sputtering on sample basal surfaces. The measurement error of electrical properties were minimalized by calibration impedance spectrometer by a calibration procedure using 100 Ω resistor. On the other hand, random errors were minimalized by performed measurement for every point at least 3 times.

3. Method

An analysis of possible mechanisms of charge carrier movement in the glass, characterized by two relaxation processes, was performed. It was done based on the frequency and temperature behavior of admittance. The analysis of admittance parameters consisted of few steps. In the first step, an equivalent electrical circuit (combined of resistors and CPEs) is proposed, which represents as many relaxation processes as are observed in a measured system. In the second step, the equation describing admittance of the equivalent circuit is used for fitting the measured data. Depending on the interesting properties of the system, equations describing Voigt (Eq. 5) or Maxwell (Eq. 6) networks can be fitted to the admittance data. For instance, using Voigt network to analyze two phases material R_1 and R_2 are resistances of these phases, while τ_1 and τ_2 – their relaxation time. It can be seen, that four parameters (i.e., A_i, R_i, τ_i and n_i) are correlated with each relaxation process. The fitting procedure is performed simultaneously on both, the real and the imaginary parts of admittance using least-squares methods (Levenberg-Marquardt algorithm) [15]. Next, obtained parameters (especially n factors) are analyzed as a function of temperature. Finally, the relations describing different conduction mechanism models are fitted to $n_i = f(T)$ function and obtained parameters are compared with the real values. All measurement data were analyzed and fitted using OrignPro9.1 software with implemented complex numbers library. Standard errors for the derived parameters were estimated according to the Error Propagation formula, which in OroginPro9.1 is an approximate formula [16].

4. Results

The obtained glass pellets were optically homogeneous, however SEM analysis shows that the material consists of two separated phases. Fig. 1 presents the SEM images of polished cross sections of the obtained pellet. In the sample uniformly dispersed phase is visible as circular granules in the matrix. Majority of dispersed granules have a diameter of about 1000 μm. An absence of XRD peaks and wide hump between 20° and 35° (Fig. 3) confirms amorphous structure of studied samples. More detailed discussion about structure of the $50MnO$ - $30SiO_2$ - $20B_2O_3$ glass has been presented in our previous paper [17].
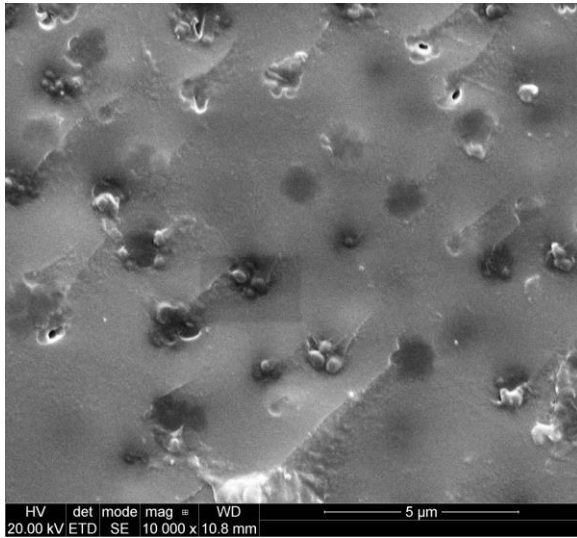
Figure 2: SEM images of cross sections of the glass at room temperature.
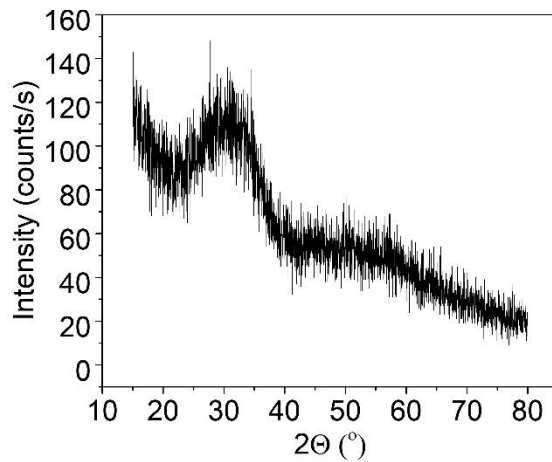

Figure 3: The XRD patterns of samples, typical of amorphous materials.

The results of admittance measured at different temperatures for the $50MnO$ - $30SiO_2$ - $20B_2O_3$ glass in a temperature range from 445 K to 745 K are presented in Fig. 2. The plots consist of three regions. One is a dc plateau dominating in a low-frequency region, which is equal to direct current conductance (Y_{dc}). Another, observed at high frequencies is a region of fast increment of conductance, where a derivative $d\ln(Y')/d\ln(f)$ changes toward 1. The last region at middle frequencies is characterized by a non-monotonic change of the data curve slope $d\ln(Y')/d\ln(f)$.
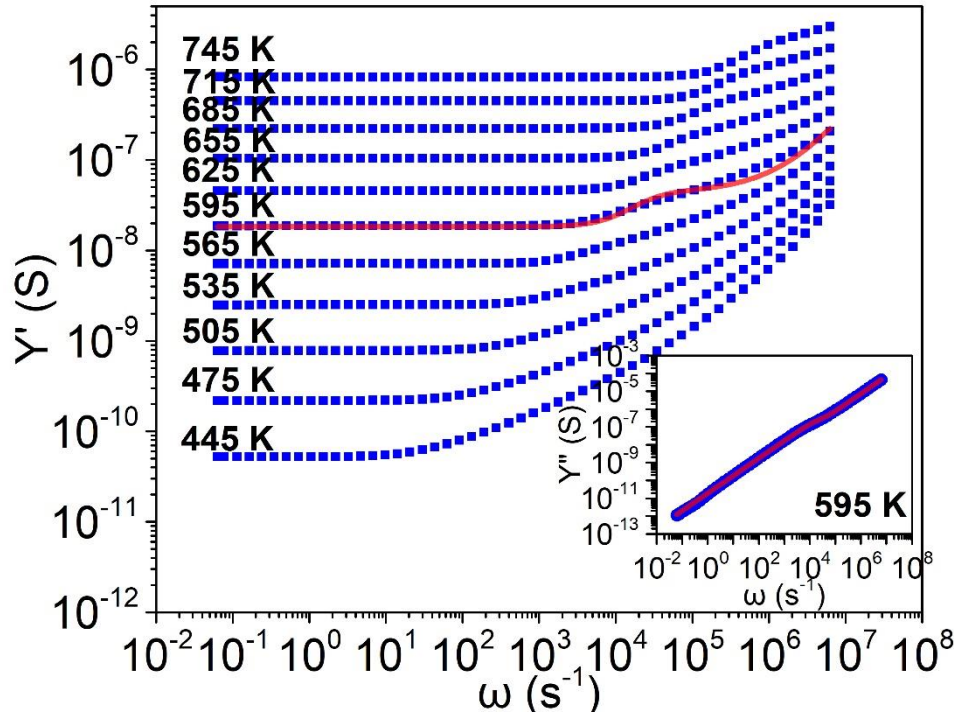
Figure 4: The conductance (and admittance in inset) for 50MnO - 30SiO$_2$ - 20B$_2$O$_3$ glass as a function of angular frequency at a temperature from 445 K to 745 K. The red lines represent the fitting results of Eq. 5 and 6, at 595 K. Error bars are smaller than a width of data points.

Table 1: Results of an equivalent circuit fitting to acquired data at temperature of 595 K. R_1 and R_2 describe resistances of the first and second relaxation processes, while τ_1, τ_2, s_1 and s_2 describe CPE_1 and CPE_2, respectively according to Eq. 5 (Voigt circuit) or Eq. 6 (Maxwell circuit). Numbers in bracket refer to a fitting error.

Model	R_1	τ_1	n_1	R_2	τ_2	n_2
	Ω	S	-	Ω	s	-
Maxwell	$5.5(1) \cdot 10^7$	$5.7(1) \cdot 10^{-5}$	0.94(1)	$7.9(4) \cdot 10^7$	$6.1(9) \cdot 10^{-5}$	0.99(1)
Voigt	$3.8(1) \cdot 10^7$	$1.4(1) \cdot 10^{-4}$	0.98(1)	$1.7(1) \cdot 10^7$	$2.1(1) \cdot 10^{-5}$	0.95(1)

As it is shown in Fig. 4, Y_{dc} value and its maximum frequency range increase with temperature. The presence of the distortion suggests that an electrical circuit appropriate to simulate the spectrum should be characterized by, at least, two relaxation processes (like shown in Fig. 1). It can be seen, that an effect of the presence of two conduction processes on the conductance spectra is better visible at 745 K than 445 K.

The data of admittance as a function of frequency and at a temperature range from 445K to 745 K, were fitted, according to the method described in section 3, to equations 5 and 6 (the conductance is shown in Fig. 2). Obtained exemplary parameters R$_1$, R$_2$, τ_1, τ_2 and n$_1$, n$_2$ for data collected at 595 K are presented in Tab. 1, while values of parameters n1 and n2 as a function of temperature are shown in Fig. 3. It can be seen, that obtained parameters for both models differ from each other by less than one order of magnitude. A similar ratio between the parameters was observed at a temperature range from 445 K to 745 K.

6

5. Discussion

The 50MnO - 30SiO$_2$ - 20B$_2$O$_3$ glass is composed of two amorphous phases, what provides a possibility to observe a few conduction processes related to conduction through the glass matrix, conduction through dispersed areas, conduction through interfaces between the matrix and the dispersed phase, and blocking of charge carriers on outer interfaces of the sample. A relaxation process related to blocking of charge carriers on electrode-sample and between phase boundaries interfaces are characterized by a long relaxation time (a few orders of magnitude higher than bulk τ) and low admittance (a few orders of magnitude lower than bulk Y) [7]. Differences between values of R_1 and R_2 (as well as between τ_1 and τ_2) (Tab. 1), describing resistances of two processes, do not exceed one order of magnitude, so they may be linked with a fast movement of charge carriers. The blocking on the internal and external interfaces is not observed, what indicates that it is not present in the measured system or that relaxation time is very low (below 10^{-2} Hz at 745 K). Consequently, to further analysis of electrical properties of the glass, the Voigt equivalent circuit characterized by two relaxation processes (Fig. 1a) was chosen.
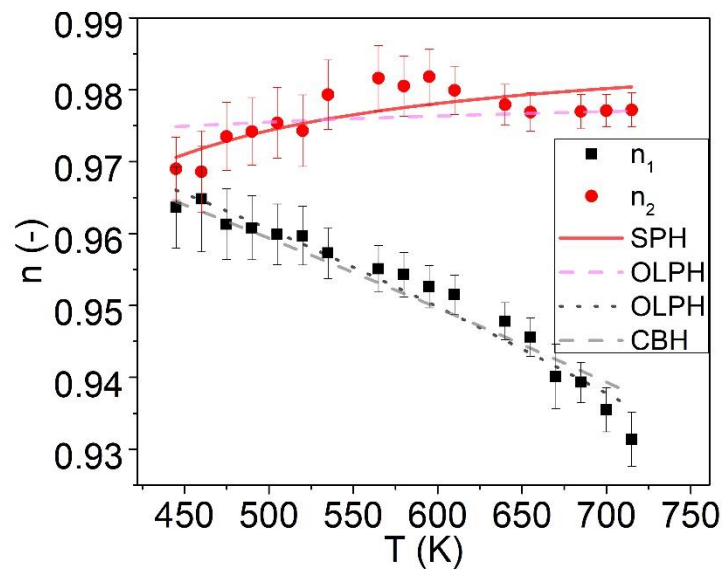

Figure 5: The n_1 and n_2 parameters obtained from admittance data fitting to equivalent Voigt circuit as a function of temperature.

The obtained values of factors n_1 and n_2 of admittance data fitted to equivalent Voigt circuit (Fig. 1a and Eq. 5) as a function of temperature are shown in Fig. 3. It can be seen, that the n_1 decreases, while n_2 slightly increases, with an increase in temperature. Elliott's [6] calculations made for several models of conduction process (i.e., SPH, OLPH, CBH, CTRW, and QMT) showed, that OLPH and CBH may be applied to describe the decrement of exponential factor n_1, while SPH, OLPH predict the increment of n_2 [6].

If we assume SPH conduction model, then n_2 parameter should change with temperature and frequency as shown in Eq. 7:

$$n = 1 - \frac{4}{\ln\left(\frac{\omega_0}{\omega}\right) - \frac{W_H}{kT}}, \qquad (7)$$

where k is Boltzmann constant, W_H an activation energy of polaron hopping barrier, and ω_0 is characteristic phonon frequency (typically $10^{12} - 10^{13}\,s^{-1}$). On the other hand, n_1 and n_2 parameters may also change according to OLPH model as shown in Eq. 8:

$$n = 1 - \frac{1}{2\alpha R_\omega} \frac{4 + 3 W_M r_0 / \alpha k T R_\omega^2}{(1 + W_M r_0 / 2\alpha k T R_\omega^2)^2}, \qquad (8)$$

or assuming CBH conduction model n_1 parameter should change as shown in Eq. 9:

$$n = 1 - \frac{6kT}{W_M - kT ln(\frac{\omega_0}{\omega})}, \qquad (9)$$

where α is an electron wave-function decay constant, r_0 - polaron radius, R_ω - tunneling distance for current frequency, and W_M an activation energy barrier of charge carrier hopping between infinitely distanced neighboring sites. Parameters W_M or W_H and $ln(\omega_0/\omega)$ (Tab. 2.) are present in all of Eq. 7-9, so they were used to compare the chosen models. As W_H in Eq. 7 does not depend on the inter-site separation length, it may be treated as well as the activation energy of hopping between infinitely distanced neighboring sites – W_M.

Table 2: Results of fitting n_1 and n_2 factors (in Voigt network) as a function of temperature according to OLPH, CBH, and SPH models. W_M or W_H and $ln(\omega_0/\omega)$ describe maximum barrier hopping energy for infinitely separated hopping sites and frequency separation between measured and phonon frequency. Numbers in bracket refer to a fitting error.

n_1	CBH	OLPH
W_M (eV)	3.1(6)	7.4(8)
$ln(\omega_0/\omega)$	11(1)	23(2)
n_2	SPH	OLPH
W_M or W_H (eV)	7(2)	0.25(5)
$ln(\omega_0/\omega)$	320(35)	21(3)

To obtain W_M or W_H and $ln(\omega_0/\omega)$ parameters, functions describing temperature dependency of the exponential factors (Eq. 8 and Eq. 9) were fitted to the data. As it can be seen in Tab. 2, W_M varies from 0.25 eV to 7.4 eV, while $ln(\omega_0/\omega)$ varies from 11 to 320. However, according to measurements performed on the glasses containing various transition metal oxides [18–20], the value of W_M is expected to be between 0.5 eV and 10 eV, while $ln(\omega_0/\omega)$ should be observed between 1 and 23. Based on these limits, one may conclude that the temperature dependency of parameter n_1 is well described by both (OLPH and CBH) models. Usefulness of both models is reasonable, as CBH and OLPH are complementary, where a macroscopic CBH may be treated as a generalization of microscopic OLPH. The obtained activation energy for OLPH is very low (0.25 eV). As the W_M should decrease when the structure becomes more ordered, one may conclude that the distance between active sites of charge carriers' movement is almost

8

regular. On the other hand, the value of $ln(\omega_0/\omega)$ above 300 obtained for SPH model cannot be treated as a physical value and the model has to be excluded.

Comparing results shown in Tab. 2, one may conclude that the values of exponential parameter n_1 obtained for Voigt equivalent circuit suits CBH or OLPH models, while parameter n_2 suits OLPH. It can be concluded, that the conduction process in the glass is carried out by hopping of large polarons through strongly disordered areas where W_M is in the order of a few eV, and through ordered areas where W_M is below 0.5 eV.

6. Conclusions

A new approach to determine conduction mechanisms in the structural amorphous materials was presented. According to the method, total admittance is separated into a few processes, which can be imitated by an equivalent electrical circuit combined with several discrete elements. Next, parameters of the equivalent circuit are fitted to experimentally gathered data in a wide range of temperature. In the end, the temperature dependency of a value of parameters describing the exponential dependency of admittance as a function of frequency according to the universal dielectric response, are compared with known theoretical models describing the conductivity behavior in amorphous systems.

This method was applied in order to identify mechanisms of conduction for $50MnO$ - $30SiO_2$ - $20B_2O_3$ (in mol%) glass sample. Based on values of resistance and relaxation time of the observed relaxation processes, it was determined that the electrical properties of the glass are properly represented by Voigt equivalent circuit characterized by two *R-CPE* sub-circuits. The analysis of the temperature dependency of exponential parameters n_1 and n_2 has shown that conduction process through the one phase (strongly disorder) can be described by correlated barrier hopping and overlapping large polarons hopping models, while conduction through the other (almost ordered) can be described by overlapping large polarons hopping models.

References

[1]   A. K. Jonscher, "*Dielectric relaxation in solids*". London: Chelsea Dielectric Press, 1983.
[2]   A. K. Jonscher, "The 'universal' dielectric response", *Nature*, vol. 267, nr 5613, pp. 673–679, 1977.
[3]   A. K. Jonscher, "A new understanding of the dielectric relaxation of solids", *J. Mater. Sci.*, vol. 16, nr 8, pp. 2037–2060, 1981.
[4]   A. K. Jonscher, "Dielectric relaxation in solids", *J. Phys. Appl. Phys.*, vol. 32, nr 14, pp. R57, 1999.
[5]   M. P. J. van Staveren, H. B. Brom, and L. J. de Jongh, "Metal-cluster compounds and universal features of the hopping conductivity of solids", Phys. Rep., vol. 208, nr 1, pp. 1–96, 1991.
[6]   S. R. Elliott, "A.c. conduction in amorphous chalcogenide and pnictide semiconductors", *Adv. Phys.*, vol. 36, nr 2, pp. 135–217, 1987.
[7]   E. Barsoukov and J. R. Macdonald, "*Impedance spectroscopy theory, experiment and Applications*", 2. New Jersey: John Wiley & Sons, 2005.
[8]   T. Holstein, "Studies of polaron motion: Part II. The "small" polaron", *Ann. Phys.*, vol. 8, nr 3, pp. 343–389, 1959.
[9]   A. R. Long, "Frequency-dependent loss in amorphous semiconductors", *Adv. Phys.*, vol. 31, nr 5, pp. 553–637, 1982.
[10] N. F. Mott, "Conduction in glasses containing transition metal ions", *J. Non-Cryst. Solids*, vol. 1, nr 1, pp. 1–17, 1968.

[11] G. E. Pike, "Ac Conductivity of Scandium Oxide and a New Hopping Model for Conductivity", *Phys. Rev. B*, vol. 6, nr 4, pp. 1572–1580, 1972.

[12] H. Scher and M. Lax, "Stochastic Transport in a Disordered Solid. I. Theory", *Phys. Rev. B*, vol. 7, nr 10, pp. 4491–4502, 1973.

[13] J. C. Dyre, "The random free-energy barrier model for ac conduction in disordered solids", *J. Appl. Phys.*, vol. 64, nr 5, pp. 2456, 1988.

[14] R. J. Barczyński, N. A. Szreder, J. Karczewski, and M. Gazda, "Electronic conductivity in the SiO_2–PbO–Fe_2O_3 glass containing magnetic nanostructures", *Solid State Ion.*, vol. 262, pp. 801–805, 2014.

[15] D.W. Marquardt, *Journal of the Society for Industrial and Applied Mathematics*, vol. 11, pp. 431–441, 1963.

[16] "Theory of Nonlinear Curve Fitting". Retrieved June 13, 2018, from https://www.originlab.com/doc/Origin-Help/NLFit-Theory

[17] P. Kupracz, J. Karczewski, M. Prześniak-Welenc, M.J. Winiarski, N. A. Wójcik, T. Klimczuk, and R. J. Barczyński ., "Microstructure and electrical properties of manganese borosilicate glasses", *J. Non-Cryst. Solids*, vol. 423–424, pp. 68–75, 2015.

[18] L. Murawski and R. J. Barczyński, "Dielectric relaxation in semiconducting oxide glasses", *J. Non-Cryst. Solids*, vol. 196, pp. 275–279, 1996.

[19] L. Murawski and R. J. Barczyński, "Dielectric properties of transition metal oxide glasses", *J. Non-Cryst. Solids*, vol. 185, nr 1–2, pp. 84–93, 1995.

[20] P. Kupracz, A. Lenarciak, M. Łapiński, M. Prześniak-Welenc, N. A. Wójcik, and R. J. Barczyński, "Polaron hopping conduction in manganese borosilicate glass", *J. Non-Cryst. Solids*, vol. 458, pp. 15–21, 2017.